

from GAG1 to LTR1, which encompasses the cleavage site, and a smaller, 200-nt fragment delineated by GAG1 and GAG2. If cleavage of *gag* RNA has occurred, a reduction in the level of the 480-nt species relative to the 200-nt fragment is expected. Untransformed cells (Fig. 4b, lanes A) contained similar levels of the 480- and 200-nt fragments, as expected. In contrast, cloned cells expressing the catalytic RNA contained significantly less of the larger, 480-nt fragment relative to the smaller, 200-nt species (lanes B). This was more striking with an RNA sample extracted from pooled clones, where the 480-nt fragment was almost undetectable (lanes C). Since the 200-nt fragment is derived from sequences not subject to cleavage, the relative reduction of this fragment in ribozyme-containing cells versus parental cells shows that the ribozyme is cleaving incoming viral RNA.

Quantitative determination of soluble p24 antigen at 7 days after infection showed a marked diminution in the amount secreted from transformed compared to parental cells. For the samples shown in Fig. 4b, the p24 concentrations were 0.14 ng/ml for cloned transformants and 0.23 ng/ml for pooled transformants. In contrast, untransformed cells secreted >10 ng/ml of the antigen. In addition to the reduction in *gag* RNA and p24 levels, HIV-1-infected, transformed cells contained significantly less (as much as 100 times) HIV-1 proviral DNA sequence compared to their infected, untransformed counterparts (21). This suggests, albeit indirectly, that constitutively expressed ribozymes can cleave incoming viral RNA genomes. A greater reduction in proviral DNA was seen in pooled compared to cloned cells (21), which correlated with the more pronounced reduction in *gag* RNA (Fig. 4b).

The potential deleterious effect of constitutively expressed catalyst on cell viability was evaluated in a short-term growth analysis. Transformed and untransformed (parental) cells were indistinguishable with respect to viability (>99% by trypan blue exclusion) and plating efficiency (>90%) at days 1, 2, 5, and 9 after seeding. The average doubling time over a 9-day period was 24.2 hours for parental cells and 23.1 hours for ribozyme-containing cells. Their RNA and DNA contents were the same and no morphological differences were detected (21). Cells expressing functional catalysts that have been in culture for more than 9 months show no signs of cytotoxicity.

Experiments presented here show stable expression of biologically active catalytic RNAs within a complex intracellular environment in the absence of cytotoxicity. Endogenous expression of an anti-*gag* catalytic

RNA caused a diminution in viral-encoded *gag* RNA, proviral DNA, and p24 antigen. That a reduction in HIV *gag* RNA occurs concomitantly with a substantial reduction (20- to 40-fold) in p24 indicates that ribozymes can affect HIV-1 replication. Although it is conceivable that cleavage is mediated by a mechanism independent of catalytic RNAs, total RNA extracted from transfected cells retains the ability to cleave HIV *gag* RNA in a cell-free system (16), indicating that cleavage can be mediated by an RNA component alone.

As with any anti-HIV-1 therapeutic strategy, the problem of a high mutability rate that may abolish the site of cleavage must be addressed. Work with oligonucleotides as inhibitors of gene expression has shown that target sequences proximal to highly conserved regions (that is, AUG translation initiation codon, splice sites, single-strand loops in hairpin structures) are more accessible to binding (22). These sites and binding sites for viral regulatory factors (that is, *tat* and *rev*), whose functions are extremely sensitive to genetic variations are logical targets for catalytic RNAs. Alternatively, a multivalent ribozyme directed to multiple cleavage sites along a single RNA transcript may increase the probability that at least one of the target sites will be cleaved. By cleaving RNA targets at specific sites, catalytic RNAs offer a means for reducing the level of deleterious RNAs. Ribozymes thus represent a newly emerging class of potential anti-HIV-1 agents. Once combined with gene therapy, the full potential of ribozymes as therapeutic agents should be realized.

REFERENCES AND NOTES

1. J. G. Izant and H. Weintraub, *Cell* **36**, 1007 (1984); R. Harland and H. Weintraub, *J. Cell. Biol.* **101**, 109 (1985); D. Melton, *Proc. Natl. Acad. Sci. U.S.A.* **82**, 144 (1985).
2. T. R. Cech and B. Bass, *Annu. Rev. Biochem.* **55**, 599 (1986).
3. J. M. Buzayan *et al.*, *Nature* **323**, 349 (1986).
4. G. A. Prody *et al.*, *Science* **231**, 1577 (1986).
5. C. J. Hutchins *et al.*, *Nucleic Acids Res.* **14**, 3627 (1986).
6. P. Keese and R. H. Symons, in *Viroids and Viroid-Like Pathogens*, J. S. Semancik, Ed. (CRC Press, Boca Raton, FL, 1987), pp. 1-47.
7. R. Tritz and A. Hampel, *Biochemistry* **28**, 4929 (1989).
8. A. C. Forster and R. H. Symons, *Cell* **49**, 211 (1987).
9. R. H. Symons, *Trends Biochem.* **14**, 445 (1989).
10. L. Epstein and J. Gall, *Cell* **48**, 535 (1987).
11. O. C. Uhlenbeck, *Nature* **328**, 596 (1987).
12. C. C. Sheldon and R. H. Symons, *Nucleic Acids Res.* **17**, 5679 (1989).
13. M. Koizumi *et al.*, *ibid.*, p. 7059.
14. J. Haseloff and W. L. Gerlach, *Nature* **334**, 585 (1988).
15. L. Ratner *et al.*, *AIDS Res. Hum. Retroviruses* **3**, 57 (1987).
16. P. S. Chang *et al.*, *Clinical Biotech.* **2**, 1 (1990).
17. P. Gunning *et al.*, *Proc. Natl. Acad. Sci. U.S.A.* **84**, 4831 (1987).
18. P. J. Maddon *et al.*, *Cell* **47**, 333 (1986).
19. R. K. Saiki *et al.*, *Science* **230**, 1350 (1985).
20. J. A. Zaia *et al.*, *J. Virol.* **62**, 3914 (1988).
21. N. Sarver *et al.*, unpublished observations.
22. J. Goodchild *et al.*, *Proc. Natl. Acad. Sci. U.S.A.* **85**, 5507 (1988).
23. G. Murakawa *et al.*, *DNA* **7**, 287 (1988).
24. We thank J. Rosenberg for his constant support; J. Chen for expert technical assistance; and M. Johnston and J. McGowan for provocative discussions and critical reading of the manuscript. Supported by a PHS, National Institute of Allergy and Infectious Diseases National Cooperative Drug Discovery Grant (AI25959) to E.C., J.Z. and J.R.; E.C., J.Z., and J.R. are members of the City of Hope Cancer Center (CA34991); P.C. was supported in part by a Medical Scientists Training Program fellowship from Loma Linda University, School of Medicine.

11 October 1989; accepted 29 December 1989

A T Cell-Specific Transcriptional Enhancer Within the Human T Cell Receptor δ Locus

JUAN MIGUEL REDONDO, SHINGO HATA,* CATHY BROCKLEHURST, MICHAEL S. KRANGEL

The T cell antigen receptor (TCR) δ gene is located within the TCR α locus. A T cell-specific transcriptional enhancer, distinct from the TCR α enhancer, has been identified within the J δ 3-C δ intron of the human T cell receptor δ gene. This enhancer activates transcription from the V δ 1 and V δ 3 promoters as well as from heterologous promoters. Enhancer activity has been localized to a 250-bp region that contains multiple binding sites for nuclear proteins. Thus, transcriptional control of the TCR δ and TCR α genes is mediated by distinct regulatory elements.

EXPRESSION OF THE REARRANGING genes that encode the immunoglobulin (Ig) and TCR polypeptides is controlled in part by promoter elements associated with the variable (V) gene segments and enhancer elements associated with the constant (C) gene segments (1).

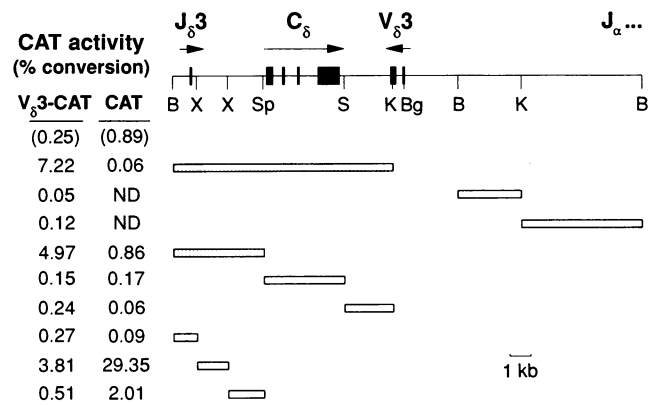
Such elements are separated by large distances in the germline configuration, but are brought into proximity by the rearrangement of V segments to diversity (D) and joining (J) segments, thereby inducing selective expression of the rearranged gene. Tissue-specific transcriptional enhancer ele-

ments have been localized upstream or downstream of the C segment for the IgM, κ , TCR β , and TCR α genes (2-8). The organization of the TCR δ locus is unique because it is located within the TCR α locus (9-11). The C δ gene segment lies upstream of the J α gene segments, roughly 100 kb from C α (9, 12-16). Most V α and V δ gene segments are located further upstream, although one V δ gene segment lies 3' of C δ (14, 16, 17). Because of the nested organization of the TCR δ and TCR α loci, the C δ region is typically deleted in lymphocytes that display V α -J α rearrangements (9, 10, 18), whereas the C α region is retained in cells that display V δ -D δ -J δ rearrangements. Thus, rearranged TCR δ genes might use the enhancer associated with the C α gene segment (7, 8). Alternatively, a specific transcriptional enhancer might be associated with the C δ gene segment and might augment transcription from rearranged TCR δ genes in T lymphocytes that bear TCR $\gamma\delta$. Selective activation of distinct TCR δ and TCR α enhancer elements could be involved in lineage determination of developing T lymphocytes.

We searched for a transcriptional enhancer within the TCR δ locus by generating a test plasmid in which a 2.5-kb Bam HI-Bgl II fragment from the 5' region of the V δ 3 gene segment served as a promoter for the expression of the chloramphenicol acetyltransferase (CAT) gene (Fig. 1). This fragment includes the transcriptional start based on the structure of a V δ 3 cDNA clone (17). This construct was essentially inactive when transfected into the human $\alpha\beta$ T cell line Jurkat and the human $\gamma\delta$ T cell line MOLT-13, indicating that additional sequences are required for expression. We then tested whether any of three DNA fragments, together spanning about 20 kb in the C δ region, could activate transcription when introduced into this construct. A 10.5-kb Bam HI-Kpn I fragment including J δ 3, C δ , and a portion of V δ 3 displayed such activity. By testing successively smaller fragments, the activity was localized to a 1.4-kb Xba I fragment mapping between J δ 3 and C δ (Fig. 1).

We generated an additional series of test constructs using the V δ 1 promoter (19). The CAT gene was activated in MOLT-13, Jurkat, or the human $\beta\delta$ T cell line DND41 (20) when the 1.4-kb Xba I fragment was inserted either upstream of the promoter or downstream of the CAT gene, in either

Fig. 1. Localization of a transcriptional enhancer within the human C δ locus. Restriction fragments from the C δ locus were cloned into the vectors V δ 3-CAT and CAT. Jurkat cells were transfected as described in Table 1. Results are reported for a single experiment in which all constructs were tested, and are expressed as percent conversion of chloramphenicol to acetylated forms. Qualitatively similar results were obtained by transfection of this series of constructs into MOLT-13 (21). The CAT vector includes a 1.9-kb Hind III-Apa I fragment of pSV2CAT, encoding the promoterless CAT gene, in the Hind III and Apa I sites of pBluescript KS+. The V δ 3-CAT vector includes, in addition, a 2.5-kb Bam HI-Bgl II V δ 3 promoter fragment in the Bam HI and Sma I sites upstream of the CAT gene. Additional fragments inserted into the two vectors are denoted by rectangles, and those that conferred activity are stippled. The initial Bam HI-Kpn I fragments to be tested were subcloned downstream of the CAT gene; fragments tested subsequently were subcloned upstream. Activities of the base constructs (V δ 3-CAT and CAT) are in parentheses. The high activity observed when the 1.4-kb Xba I fragment is immediately upstream of the promoterless CAT gene may reflect promoter activity of this fragment that is revealed once flanking sequences are removed. B, Bam HI; X, Xba I; S, Sac I; K, Kpn I; Sp, Sph I; Bg, Bgl II; ND, not determined.



orientation (Fig. 2A and Table 1). This activation was equivalent to that induced by the 10.5-kb Bam HI-Kpn I fragment (21), and was similar in magnitude to that induced using a strong heterologous enhancer fragment (RSVE) isolated from the Rous sarcoma virus (RSV) long terminal repeat (LTR) (Table 1). Activity depended on the presence of both the promoter and enhancer, since the CAT-1.4r construct displayed low activity relative to V δ 1-CAT-1.4r (Fig. 2A). The 1.4-kb fragment may contain promoter activity as well, since the CAT gene was more active when the fragment was cloned immediately upstream, rather than downstream, of the CAT gene (Fig. 1) (21).

The 1.4-kb Xba I fragment was also capable of activating transcription in constructs carrying a minimal simian virus 40 (SV40) early region promoter or the *c-fos* promoter (Fig. 2B and Table 1). In contrast, the 1.4-kb Xba I fragment was slightly inhibitory with any of these promoters in the human epithelial carcinoma cell line HeLa, the human Epstein-Barr virus-transformed B lymphoblastoid cell line X50-7, and the human Burkitt's lymphoma Raji (Table 1). For unknown reasons, the fragment was only weakly active in some additional T cell lines (22). We conclude that the 1.4-kb Xba I fragment carries a tissue-specific transcriptional enhancer that is active in at least some $\gamma\delta$ and $\alpha\beta$ T cell lines.

To delineate the region of the 1.4-kb Xba I fragment responsible for enhancer activity, we generated a series of constructs with progressive deletions from the 5' end of this fragment in the plasmid 1.4-V δ 1-CAT, and a similar series of deletions from the 5' end

of this fragment in the reverse orientation in the plasmid 1.4r-V δ 1-CAT. Enhancer activity was assayed after transfection into MOLT-13 (Fig. 3). In parallel, these constructs were used to determine the nucleotide sequence of the 1.4-kb Xba I fragment. Maximal enhancer activity was localized to a 250-bp segment near the 3' end of the fragment (in the natural orientation). The adjacent 400-bp region may carry a weak negative element, as deletion of this segment consistently resulted in a small increase (up to two times) in enhancer activity.

We analyzed the sites within the enhancer region that interact with specific nuclear

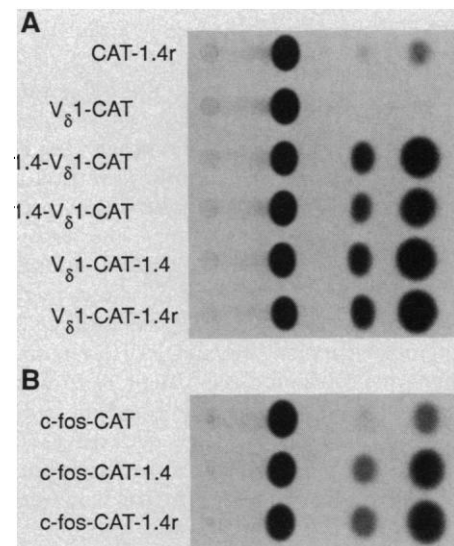


Fig. 2. Enhancer activity of the 1.4-kb Xba I fragment in MOLT-13 cells. (A) Activation of V δ 1-CAT. (B) Activation of *c-fos*-CAT. Constructs, transfections, and assays are as described in Table 1.

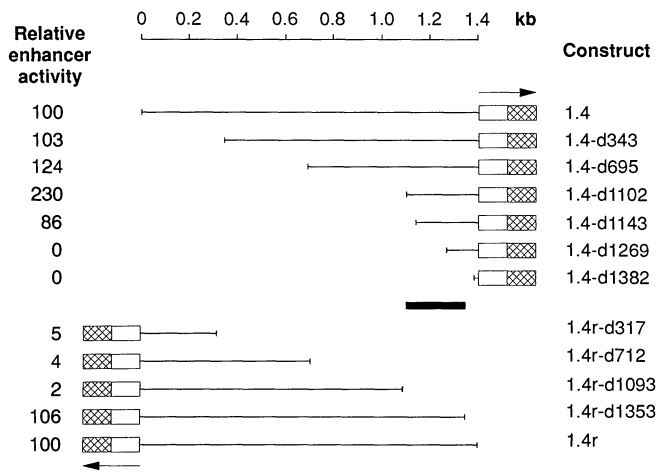
Division of Tumor Virology, Dana-Farber Cancer Institute, Harvard Medical School, Boston, MA 02115.

*Present address: Laboratory of Chemical Tolerance, Department of Applied Physiology, National Institute of Agrobiological Resources, 2-1-2 Kannondai, Tsukuba, Ibaraki 305, Japan.

proteins by DNase I footprinting. For these studies we used a 370-bp fragment extending from a Dra I site at nucleotide 1030 to the 3' end of the 1.4-kb fragment, and two smaller fragments, of 210 and 160 bp, that were generated by digestion of the 370-bp fragment at an Nsi I site at nucleotide 1240. Seven discrete regions ($\delta E1$ to $\delta E7$) bound factors in MOLT-13 and Jurkat nuclear extracts (Fig. 4, A and B). All seven regions were footprinted on both strands by both extracts yielding a reproducible pattern of protected and hypersensitive nucleotides. Although the footprints over $\delta E1$ and $\delta E2$ are subtle, the observation that deletion of these sites results in a 63% drop in enhancer activity (Figs. 3 and 4B) confirms that they represent binding sites for nuclear factors. Initial experiments with B cell nuclear extracts showed much weaker or in some cases altered footprints at sites $\delta E1$ to $\delta E7$ (Fig. 4A) (21).

The protected regions are characterized by a number of sequence motifs (Fig. 4B, arrows): an inverted repeat of the sequence TGTATTATTT in $\delta E1$, a direct repeat of the sequence TTGTAAC in $\delta E2$, an inverted repeat of the sequence TGGTTTCC shared by $\delta E3$ and $\delta E5$, a direct repeat of the sequence GTTATCA in $\delta E4$, and a direct repeat of the sequence AAGCAGGTT in $\delta E6$. Further, some protected sequences are similar to regions that may be important in

Fig. 3. Localization enhancer activity within the 1.4-kb Xba I fragment. A series of 5' deletions were introduced into the Sac I plus Not I-digested plasmids 1.4-V₈I-CAT and 1.4r-V₈I-CAT with exonuclease III; plasmids were then recircularized with Klenow and T4 DNA ligase (Erase-a-Base, Promega). Deletion end points were determined by nucleotide sequence analysis, and enhancer activity was assessed after transfection into MOLT-13. Enhancer activity within each series of deletions is expressed as the percent of activity displayed by the parent construct. The region displaying maximal activity is denoted by the filled rectangle.



other enhancer elements (Fig. 4C): segments of the T α 1, T α 2, and T α 3 elements of the human TCR α enhancer (8); the $\kappa E3$ element of the Ig κ enhancer (23); the $\mu E1$ and $\mu E3$ elements of the Ig heavy chain enhancer (23, 24); the viral core consensus sequence (25); and an interferon consensus sequence (26). Thus, some of the nuclear factors that bind to the TCR δ enhancer may be related or identical to factors that bind to other enhancer elements. It is not yet certain which of the protected regions are important in mediating tissue-specific enhancer activity, or the identities of the proteins that

interact with these sites. However, our initial series of deletion constructs indicate that $\delta E1$, $\delta E2$, and $\delta E7$ probably make relatively small contributions to enhancer activity, whereas $\delta E3$ may be essential (Figs. 3 and 4).

The human TCR α enhancer is active in the human $\alpha\beta$ T cell line Jurkat, but inactive in the human $\gamma\delta$ T cell lines MOLT-13 and PEER (8). Lineage-specific activity of the murine TCR α enhancer has been attributed to nearby silencers that inactivate the enhancer in $\gamma\delta$ T cell as well as non-T cell lines (27). These observations argue that a dis-

Table 1. Activity of the 1.4-kb Xba I fragment. Suspension cells (10^7) or approximately 2×10^6 HeLa cells were transfected in a 16- to 20-hour incubation with CsCl purified plasmid DNA (2 μ g) and Lipofectin (BRL) (5 μ g) in 1 ml of OptiMEM (Gibco). DND41 was transfected with five times more DNA and Lipofectin. Cell extracts were prepared after 48 hours and were assayed for acetylation of [¹⁴C]chloramphenicol (32) during a 4-hour incubation period. Acetylation was quantified by thin-layer chromatography followed by analysis with a Betascope (Betagen). Results are presented for a series of representative experiments and are expressed as percent conversion of chloramphenicol to acetylated forms. The standard deviation of determinations performed in triplicate in a single experiment averaged 10.5% of the mean, indicating that absolute and relative determinations within an experiment were highly reliable. In making the V₈I-CAT constructs we used a 1.6-kb Hind III-Bam HI fragment of pSV2CAT (32) cloned into the Hind III and Xho I sites of pBluescript KS+ (Stratagene). The V₈I promoter fragment was in the Sma I site upstream of the CAT gene, and the 1.4-kb Xba I fragment was either upstream (in the Bam HI site) or downstream (in the Kpn I site) in either orientation (1.4 and 1.4r). SVp-CAT carries a 155-bp Fok I-Hind III fragment of the SV40 promoter (including one complete and one partial 21-bp repeat) between the Eco RV and Hind III sites upstream of the CAT gene. The 1.4-kb Xba I fragment was in the Not I site upstream of the promoter in either orientation. The *c-fos*-CAT plasmid was J21 (7). The 1.4-kb Xba I fragment was in either orientation in the Eco RV site 2.5 kb downstream of the promoter. The RSVE, a 300-bp Eco RI-Nru I fragment of the RSV LTR (33), was in the Kpn I site downstream of the CAT gene. Ep, epithelial cells.

Plasmid	CAT activity (% conversion) in the cell lines										
	MOLT-13 (T $\gamma\delta$)			Jurkat (T $\alpha\beta$)			DND41 (T $\beta\delta$)		HcLa (Ep)	X50-7 (B)	Raji (B)
	Expt. 1	Expt. 2	Expt. 3	Expt. 1	Expt. 2	Expt. 3	Expt. 1	Expt. 2	Expt. 1	Expt. 1	Expt. 1
V ₈ I-CAT	0.15	0.31	0.12	0.19	0.30	0.12	0.16	0.10	0.33	0.20	
1.4-V ₈ I-CAT	39.76	8.07	8.46	9.87	9.04	3.17	8.17	2.76	0.10	0.10	
1.4r-V ₈ I-CAT	22.36			3.10	4.22			0.75			
V ₈ I-CAT-1.4	46.13			3.14	3.40			2.60			
V ₈ I-CAT-1.4r	61.01	12.38	15.12	6.71	5.91	1.49		6.31			
V ₈ I-CAT-RSVE		11.20	40.27			5.24					
SVp-CAT	0.45	0.15	0.35	3.68	4.54				2.03	0.75	1.60
1.4-SVp-CAT	1.82	0.69	1.28	8.77	14.46				0.70	0.40	0.85
1.4r-SVp-CAT	2.96	2.30		13.82	21.92				1.02	0.36	
<i>c-fos</i> -CAT	6.50	1.79	0.54	4.71	5.61		0.43		20.16	33.68	7.06
<i>c-fos</i> -CAT-1.4	32.92	25.04	9.33	36.11	32.15		3.82		8.69	16.22	4.84
<i>c-fos</i> -CAT-1.4r	49.01			46.02			6.89				

tinct enhancer might be required to activate transcription from rearranged TCR δ genes. We have identified a transcriptional enhancer located within the J δ 3-C δ intron of the TCR δ locus that is active in two T cell lines that express a rearranged TCR δ gene, MOLT-13 and DND41, suggesting that it might function to activate transcription from rearranged TCR δ genes in vivo. This

enhancer is also active in the human $\alpha\beta$ T cell line Jurkat, even in the context of a large genomic fragment extending 2 kb 5' and 8 kb 3' of the TCR δ enhancer (Fig. 1). Thus, we have no evidence for nearby, lineage-specific silencers as described for the TCR α enhancer (27). Given these results with a limited number of leukemic T cell lines, it is difficult to draw firm conclusions regarding

the tropism of this enhancer within the T cell lineage. Nevertheless, it would appear that the trans-acting factors that activate the TCR δ enhancer are not expressed in a strictly lineage-specific fashion.

Conflicting data have been obtained regarding the issue of whether TCR $\gamma\delta$ and TCR $\alpha\beta$ lymphocytes arise stochastically as the products of successive rearrangements at the TCR α/δ locus, or alternatively, arise as distinct lineages that are competent for TCR δ rearrangement or TCR α rearrangement, but not both (18, 28, 29). Since the onset of rearrangement at a locus appears to be closely associated with transcriptional activation (30, 31), it is possible that activation of the TCR δ enhancer may direct TCR δ gene rearrangements in developing T lymphocytes. If so, the presence of trans-acting factors that activate the TCR δ enhancer in TCR $\alpha\beta$ lymphocytes, which have deleted the entire C δ region including the enhancer, may be indicative of initial activation of the TCR δ locus before V α to J α rearrangement. This would be consistent with a model of progressive rearrangement at the TCR α/δ locus. Thus, the D δ and J δ segments would initially be activated for rearrangement by trans-acting factors interacting with the TCR δ enhancer. In the absence of rearrangement, or failing productive rearrangement and expression of a cell surface $\gamma\delta$ TCR, the TCR α enhancer would be derepressed, allowing subsequent rearrangements to J α [or ψ J α (18)] segments to occur. TCR $\alpha\beta$ lymphocytes arising by this pathway might therefore express residual trans-acting factors capable of interacting with the TCR δ enhancer, even though the enhancer itself had been previously deleted.

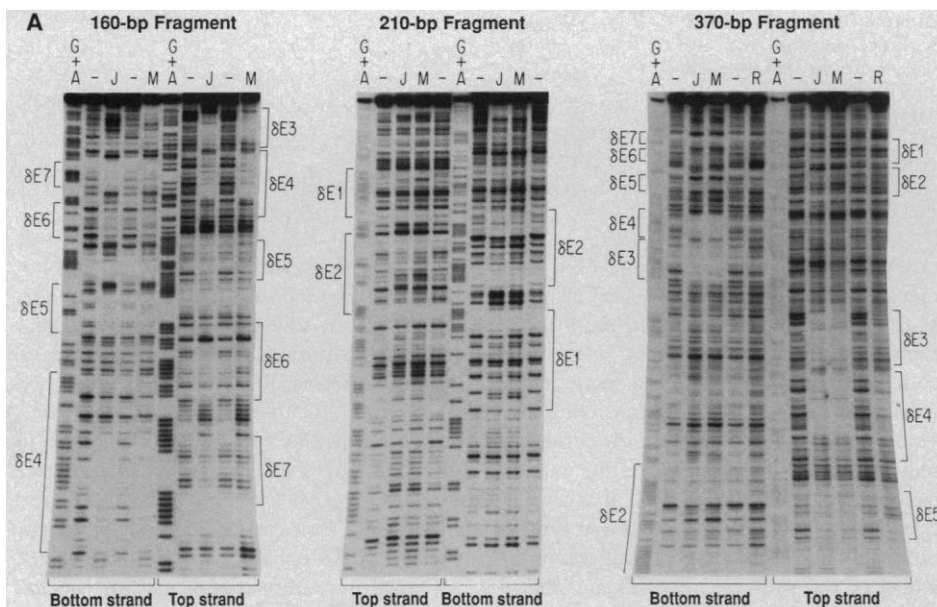
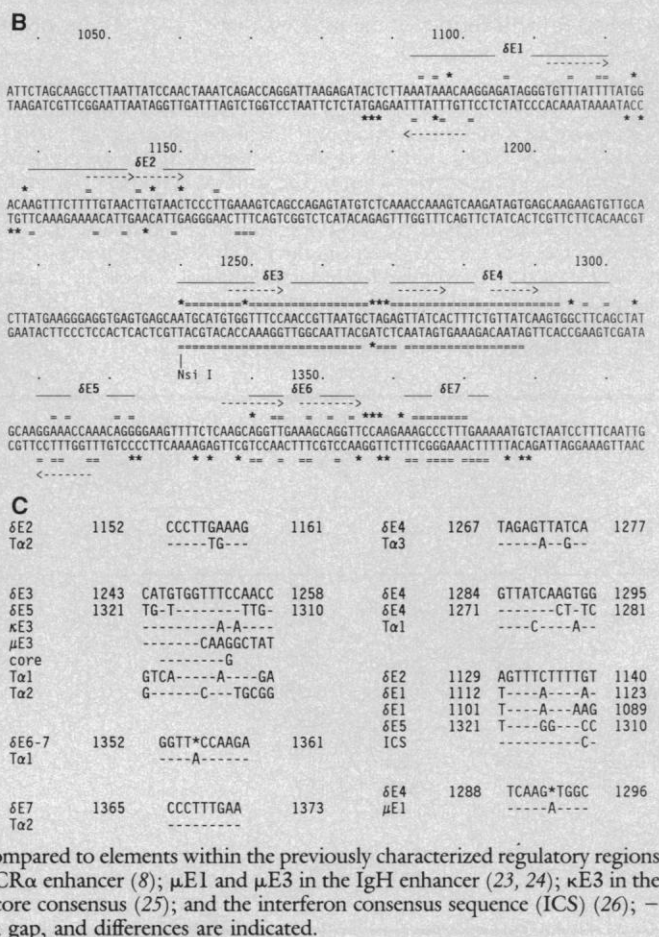


Fig. 4. Protein binding sites within the TCR δ enhancer. **(A)** A 160-bp Nsi I-Xba I fragment, a 210-bp Dra I-Nsi I fragment, and a 370-bp Dra I-Xba I fragment spanning the enhancer region were analyzed by DNase I footprinting with MOLT-13, Jurkat, and Raji nuclear extracts, as described (34, 35). G+A, standard Maxam-Gilbert G+A reaction; -, no nuclear extract; J, 200 μ g of Jurkat nuclear extract; M, 100 μ g of MOLT-13 nuclear extract; R, 100 μ g of Raji nuclear extract. The regions bracketed correspond to putative protein binding sites as overlined in (B). **(B)** The nucleotide sequence was determined on both strands with deletion plasmids as templates. Protected nucleotides are denoted by =, hypersensitive nucleotides are denoted by *, protein binding regions are denoted by solid overlines, and repeat elements are denoted by ---. **(C)** Sequences within the footprinted regions are compared to elements within the previously characterized regulatory regions Ta1, Ta2, and Ta3 in the TCR α enhancer (8); μ E1 and μ E3 in the IgH enhancer (23, 24); κ E3 in the Ig κ enhancer (23); the viral core consensus (25); and the interferon consensus sequence (ICS) (26); - denotes identity, * denotes a gap, and differences are indicated.



REFERENCES AND NOTES

1. K. Calame and S. Eaton, *Adv. Immunol.* **43**, 235 (1988).
2. S. D. Gillics, S. L. Morrison, V. T. Oi, S. Tonegawa, *Cell* **33**, 717 (1983).
3. S. Banerji, L. Olson, W. Schaffner, *ibid.*, p. 729.
4. D. Picard and W. Schaffner, *Nature* **307**, 80 (1984).
5. P. Krimpenfort *et al.*, *EMBO J.* **7**, 745 (1988).
6. S. McDougall, C. L. Peterson, K. Calame, *Science* **241**, 205 (1988).
7. A. Winoto and D. Baltimore, *EMBO J.* **8**, 729 (1989).
8. I.-C. Ho, L.-H. Yang, G. Morle, J. M. Leiden, *Proc. Natl. Acad. Sci. U.S.A.* **86**, 6714 (1989).
9. Y.-H. Chien, M. Iwashima, K. B. Kaplan, J. F. Elliott, M. M. Davis, *Nature* **327**, 677 (1987).
10. S. Hata, M. B. Brenner, M. S. Krangel, *Science* **238**, 678 (1987).
11. E. Y. Loh *et al.*, *Nature* **330**, 569 (1987).
12. M. Isobe, G. Russo, F. G. Haluska, C. M. Croce, *Proc. Natl. Acad. Sci. U.S.A.* **85**, 3933 (1988).
13. Y. Takihara *et al.*, *ibid.*, p. 6097.
14. K. Satyanarayana *et al.*, *ibid.*, p. 8166.
15. R. D. Hockett *et al.*, *ibid.*, p. 9698.
16. E. Y. Loh, S. Swirl, A. T. Scrafin, J. H. Phillips, L. Lanier, *ibid.*, p. 9714.
17. S. Hata *et al.*, *J. Exp. Med.* **169**, 41 (1989).
18. J.-P. de Villartay, R. D. Hockett, D. Coran, S. J. Korsmeyer, D. I. Cohen, *Nature* **335**, 170 (1988).

19. The $V_{\beta}1$ promoter fragment was generated by exonuclease III digestion. It extends from -1544 to +18 relative to the transcription start site as determined by S1 nuclease mapping. Activity of the $V_{\beta}1$ promoter appears to be T cell-specific based on its stimulation of CAT activity when introduced upstream of the CAT gene in the vector CAT-RSVE.
20. F. Hochstenbach and M. B. Brenner, *Nature* **340**, 562 (1989).
21. J. M. Redondo and M. S. Krangel, unpublished results.
22. Activation by the RSVE fragment was also weak in these T cell lines. Thus, weak activation by the 1.4-kb Xba I fragment may reflect factors other than its intrinsic activity.
23. R. Sen and D. Baltimore, *Cell* **46**, 705 (1986).
24. A. Ephrussi, G. M. Church, S. Tonegawa, W. Gilbert, *Science* **227**, 134 (1985).
25. P. Sassone-Corsi and E. Borrelli, *Trends Genet.* **2**, 215 (1986).
26. Y. Shirayoshi, P. A. Burke, E. Appella, K. Ozato, *Proc. Natl. Acad. Sci. U.S.A.* **85**, 5888 (1988).
27. A. Winoto and D. Baltimore, *Cell* **59**, 649 (1989).
28. ———, *Nature* **338**, 430 (1989).
29. S. Takeshita, M. Toda, H. Yamagishi, *EMBO J.* **8**, 3261 (1989).
30. F. W. Alt, T. K. Blackwell, G. D. Yancopoulos, *Science* **238**, 1079 (1987).
31. M. Schliessel and D. Baltimore, *Cell* **58**, 1001 (1989).
32. C. M. Gorman, L. F. Moffat, B. H. Howard, *Mol. Cell. Biol.* **2**, 1044 (1982).
33. P. A. Luciw, J. M. Bishop, H. E. Varmus, M. R. Capecchi, *Cell* **33**, 705 (1983).
34. J. D. Dignam, R. M. Lebovitz, R. G. Roeder, *Nucleic Acids Res.* **11**, 1475 (1983).
35. W. Lee, P. Mitchell, R. Tjian, *Cell* **49**, 741 (1987).
36. We thank C. Doyle, S. Speck, E. Flemington, M. Woisetschlaeger, D. Diamond, A. Winoto, R. Guigo, and B. Alarcon for contributing reagents and for helpful discussions. Supported by a grant from NIH (R01-GM41052) and a Doctores y Tecnologos fellowship from the Ministerio de Educacion y Ciencia Español (to J.M.R.).

21 November 1989; accepted 6 February 1990

The Direction of Membrane Lipid Flow in Locomoting Polymorphonuclear Leukocytes

JULIET LEE, MIKAEL GUSTAFSSON, KARL-ERIC MAGNUSSON, KEN JACOBSON*

The objective of this study was to determine the direction of membrane lipid flow in locomoting cells. The plasma membrane of human polymorphonuclear leukocytes was stained with a fluorescent lipid analog dihexadecanoyl indocarbocyanine. A line was photobleached on the cell surface perpendicular to the direction of cell motion. Low-light-level fluorescence microscopy and digital image-processing techniques were used to analyze a series of images taken at short intervals after photobleaching. The bleached line remained visible for about 5 seconds before being erased by diffusional recovery. Examination of fluorescence intensity profiles allowed a comparison to be made between the velocities of line and cell movement. Results indicate that the bleached line moves forward with the same velocity as the cell during locomotion, refuting the retrograde lipid flow model of locomotion. Instead, the plasma membrane lipid appears to move forward according to either the unit movement of membrane or the tank track model of locomotion.

A KEY TO UNDERSTANDING THE MOLECULAR basis of cell locomotion lies in investigating the dynamics of membrane and cytoskeletal molecules during cell movement. Early approaches to this problem revealed the rearward movement of particles attached to the surface of moving cells (1). Patched or cross-linked membrane proteins were also found to display the same behavior in motile cells, the most familiar example being the phenomenon of capping (2). Recent advances in the field of digitized video microscopy permit the dynamics of well-characterized classes of proteins to be

visualized in locomoting cells over extended periods of time (3–5), including the rearward movement of specific fluorescently labeled membrane proteins (6, 7). Submicron gold particles coated with either lectins, polylysine, or monoclonal antibodies have also been used to track the movements of membrane constituents (8–10).

Information about the movement of membrane components has been used to support several very different models of cell locomotion (11–13). These models differ on how the forces underlying membrane protein movement and cell locomotion are generated. The idea that the cytoskeleton is responsible for the rearward movement of membrane proteins (13–15) is supported by a considerable amount of experimental evidence (2, 5, 7, 16, 17). This cytoskeletal-driven process is regarded as part of the locomotory mechanism. Thus, it may be envisaged that when rearward-moving

membrane proteins on the ventral cell surface become anchored to the substratum, continuation of a rearward-directed cytoskeletal force will tend to pull the cell forward.

An alternative explanation for the rearward movements of membrane proteins is the retrograde lipid flow (RLF) hypothesis (12). In this model, which has previously been used to explain the rearward movements of particles on the surface of moving cells (1), a rearward lipid flow exists on the dorsal and ventral cell surfaces that sweeps slowly diffusing membrane proteins or attached particles from the front to the rear of the cell. A rearward lipid flow is thought to be generated by the insertion of new membrane lipid (source) at the tip of the leading lamella, and the endocytosis of membrane lipid (sink) at sites randomly distributed over the cell surface. The cell is thought to advance by inserting new membrane lipid at the tip of the extending lamella. However, there has been no direct information about the direction of lipid flow in locomoting cells. All information regarding flow has been inferred from studies of particle movement on the surface of motile cells (1, 9). Therefore, an essential step toward building more realistic models of cell locomotion is to determine the direction of lipid flow directly in moving cells.

We have developed a method to detect the direction of plasma-membrane lipid flow during cell locomotion. We trace the movement of a mark created by photobleaching fluorescent lipid molecules embedded in the membrane of moving cells. A fluorescent lipid analog, dihexadecanoyl-indocarbocyanine (diI), was used to stain the membrane lipid of human polymorphonuclear leukocytes (PMNs). A pulse of laser light was then used to destroy the fluorescence within a discrete band across the cell, perpendicular to its direction of motion. Movement of the bleached line was recorded at short intervals after photobleaching (Fig. 1). However, this line is only temporary, since it is rapidly erased (within 5 s) by diffusion of unbleached fluorophores into the bleached region. Thus, the success of the experiment depends heavily on the degree of cell motility. Only in rapidly moving cells can line movement be detected before diffusional recovery is complete. Human PMNs are particularly suitable for this study as they can be highly motile on a glass substratum after staining with diI and are resilient to the effects of photobleaching in the presence of diI. A single cell may be photobleached up to five times without any apparent impairment of cell mobility or viability. One concern about this procedure is that membrane-bound diI is gradually internalized. Thus

J. Lee and K. Jacobson, Department of Cell Biology and Anatomy and Lineberger Cancer Research Center, University of North Carolina at Chapel Hill, Chapel Hill, NC 27599.

M. Gustafsson and K.-E. Magnusson, Department of Medical Microbiology, University of Linköping, Linköping, Sweden.

*To whom correspondence should be addressed.